

C.P. No. 1249



LIBRARY  
DEFENCE  
BEDFORD.

C.P. No. 1249

PROCUREMENT EXECUTIVE, MINISTRY OF DEFENCE

AERONAUTICAL RESEARCH COUNCIL

CURRENT PAPERS

Wind-Tunnel Force Measurements  
on a 1/20 Scale Model of  
Black Arrow at Mach Numbers  
of 1.2, 1.5 and 2.0

by

J R. Hall

*Aerodynamics Dept., R.A.E., Bedford*

LONDON: HER MAJESTY'S STATIONERY OFFICE

1973

PRICE 55p NET



UDC 629.192.21 : 533.6.013.11 : 533.6.071 : 533.6.011.5

CP No.1249\*

March 1972

WIND TUNNEL FORCE MEASUREMENTS ON A 1/20 SCALE MODEL OF BLACK ARROW  
AT MACH NUMBERS OF 1.2, 1.5 AND 2.0

by

J. R. Hall

SUMMARY

The forces measured on a 1/20 scale model of Black Arrow at Mach numbers of 1.2, 1.5 and 2.0 and at a Reynolds number, based on the maximum body diameter, of  $1.31 \times 10^6$  are presented. The effects of the external fittings are deduced and the results are discussed.

---

\* Replaces RAE Technical Report 72061 - ARC 34019

CONTENTS

	<u>Page</u>
1 INTRODUCTION	3
2 MODEL DETAILS	3
3 TEST DETAILS	4
3.1 Coordinate system and coefficients	4
3.2 Description of tests	4
3.3 Transition fixing	4
3.4 Data reduction	5
3.5 Accuracy of the results	5
4 DISCUSSION OF RESULTS	6
5 CONCLUSIONS	8
Symbols	10
References	11
Illustrations	Figures 1-18
Detachable abstract cards	

Neg. C 8895

## 1 INTRODUCTION

Black Arrow was a three-stage satellite launcher based for economic reasons on Black Knight technology and equipment. In its originally conceived form<sup>1</sup>, as tested here, it was expected to have the capability of launching a satellite of at least 160 lb into a 300 nm circular polar orbit. Subsequent development of the basic launcher resulted in an appreciable increase in its performance<sup>2</sup> and a version using 'wrap-round' booster rockets on the first stage was also considered<sup>3</sup>.

This Report presents the results of five-component balance measurements (no axial force) made on a 1/20 scale model of Black Arrow at Mach numbers of 1.2, 1.5 and 2.0 in the RAE 8ft x 8ft supersonic wind tunnel at Bedford during May 1965. The tests were carried out at a Reynolds number, based on the maximum body diameter, of  $1.31 \times 10^6$ . Complementary subsonic and transonic testing was carried out in the 8ft x 6ft transonic wind tunnel at RAE Farnborough using the same model and balance.

In addition to the overall static aerodynamic characteristics of the launcher, the tests were designed to determine the effects of the external pipes and fairings. For this reason two configurations were tested; configuration 01 was a 'clean' axisymmetric model having no external excrescences and configuration 02 was complete with various external pipes and fairings representing the full-scale launcher in some detail.

## 2 MODEL DETAILS

A view of the model in the wind tunnel is presented in Fig.1. The model was constructed mainly in aluminium alloy in the workshops at RAE Farnborough. It consists of an axisymmetric forebody and afterbody joined by a steel centre section embodying an integral adaptor for the balance. This basic shape was machined to take either a set of blank inserts which gave a smooth axisymmetric model - configuration 01 - or a set of inserts (some of which are visible in Fig.1) on which were mounted various pipes and fairings - configuration 02. Details of the model and the fittings are given in Figs.2a and 2b respectively.

The model was mounted on a five-component integral sting - balance (RAE Farnborough balance SB 527) and was instrumentated to record base pressure using a CEC pressure transducer.

### 3 TEST DETAILS

#### 3.1 Coordinate system and coefficients

The coordinate system adopted is shown in Fig.3, being such that the axes move with the model in pitch but not in roll (resolved body axes). The model roll datum (XX in Fig.2a) is taken to be defined by the position of the shortest external pipes and the smallest fairing near the base of the model and the moment reference point (O in Fig.3) is taken to be at the intersection of the model axis with the plane YY (see Fig.2a) through the junction of the flare and the forebody. The measured forces, moments and pressures are non-dimensionalised using the free-stream kinetic pressure, the maximum diameter and the maximum cross-sectional area of the axisymmetric body (see list of symbols).

#### 3.2 Description of tests

The model was mounted on a sting (Fig.1) from the quadrant of the 8ft  $\times$  8ft wind tunnel and tests were carried out at nominal Mach numbers of 1.2, 1.5 and 2.0 at a constant Reynolds number per foot of  $4 \times 10^6$ . The resulting Reynolds number based on the maximum body diameter,  $R_d$ , was  $1.31 \times 10^6$ , which was an order of magnitude less than the estimated full-scale flight Reynolds number (Fig.4).

Balance and pressure-transducer readings were taken at intervals of  $1^\circ$  between  $-10^\circ$  and  $+10^\circ$  with additional points every  $\frac{1}{2}^\circ$  between  $0^\circ$  and  $+3^\circ$ . These nominal incidences were set on a comparator and the readings were stored and recorded automatically as the model was swept slowly from  $-11^\circ$  to  $+11^\circ$ .

Incidence sweeps were taken at roll angles of both  $\phi = 0^\circ$  and  $90^\circ$  for configuration 01, in order to provide a check on symmetry, and at roll angles every  $15^\circ$  between  $-90^\circ$  and  $+90^\circ$  for configuration 02.

For configuration 02, at  $\phi = 0^\circ$ ,  $45^\circ$  and  $90^\circ$  and  $M = 1.2$ , incidence sweeps were also taken for Reynolds numbers per foot of  $3 \times 10^6$  and  $5 \times 10^6$  ( $R_d = 0.98 \times 10^6$  and  $1.64 \times 10^6$ ).

#### 3.3 Transition fixing

A transition band 0.15 inch wide consisting of a sparse distribution of ballotin 0.007-0.008 inch in diameter was attached 0.8 inch behind the nose of the model (Fig.1). The criteria put forward in Ref.4 suggest that transition occurred at, or just behind, the roughness band at all test conditions.

### 3.4 Data reduction

The force measurements were corrected for first-order balance interactions and the values of model incidence,  $\theta$ , were corrected for model deflections. For the results at  $M = 1.2$  a further correction to the measured values of incidence was necessary to account for flow misalignment in the wind tunnel. This correction was deduced from the measurements on configuration 01, by forcing the curves of  $-C_Z$  versus  $\theta$  to pass through the origin, and amounted to:

$R_d \times 10^{-6}$	0.98	1.31	1.64
$\Delta\theta$	$-0.15^\circ$	$-0.05^\circ$	$-0.15^\circ$

The true test Mach numbers, after correction for the effects of tunnel total pressure and temperature, were:

$R_d \times 10^{-6}$	$M_N$	$M$
0.98	1.2	1.202
1.64	1.2	1.212
1.31	1.2	1.207
1.31	1.5	1.505
1.31	2.0	2.006

### 3.5 Accuracy of the results

The majority\* of the measured coefficients and centres of pressure are estimated to be accurate to within:

$$\begin{aligned}
 -C_Z, C_Y &\pm 0.005 \\
 C_m, C_n &\pm 0.007 \text{ (includes an allowance of 0.004} \\
 &\text{for flow curvature in the tunnel)} \\
 C_l &\pm 0.002 \\
 \theta, \phi &\pm 0.05 \\
 X_{cp}/d &\pm 0.05
 \end{aligned}$$

These estimates take account of errors due to balance calibration and hysteresis, to tunnel calibration and flow curvature, to time drifts and to the resolution of the recording system used. The error in the predicted trends of any individual coefficient during an incidence sweep is believed to be well within these limits.

---

\* The pitching moment data contained a particularly large number of rogue points and points which - if the aerodynamics are smooth - lie outside the above estimates of accuracy (see Figs.10-13). These latter points, although presented, have been treated as spurious and have not been included in the discussion of the results.

These errors are larger than generally expected in the 8ft  $\times$  8ft wind tunnel due mainly to the fact that, for the sake of speed of manufacture and testing, the model was built around an existing low-stress balance.

#### 4 DISCUSSION OF RESULTS

The normal force coefficients,  $-C_z$ , for the axisymmetric configuration 01 are presented in Fig.5 and show that there is no measurable asymmetry in the results either from rotating the model through  $90^\circ$  of roll,  $\phi$ , or from pitching the model through positive and negative values of incidence,  $\theta$ . The normal force coefficients for both configurations are presented in Figs.6-8. The addition of the external fittings results in a small increase in the normal force coefficients, and in the initial slope of the normal force curve, at all test conditions. The values of the initial slope of the normal force curves for both configurations were obtained graphically and are presented in Fig.9. The increase in normal force is a maximum with the pipes nearest to the horizontal plane, i.e.  $\phi \approx -5^\circ$ , and there is little increase over a broad range of roll angles with the pipes near the vertical plane, i.e.  $60^\circ < |\phi| < 120^\circ$ . This suggests that the effects of the fairings are small compared to the effects of the pipes. This is to be expected because, though they project further from the surface, their projected area normal to the surface is only 19% of that of the pipes. As expected there are no measurable differences between the normal force coefficients at positive and negative values of  $\theta$ , since the only asymmetry is due to the small fairing nearest to the base of the model (Fig.2).

The pitching moment coefficients,  $C_m$ , for the axisymmetric configuration 01 are presented in Fig.10 and show that, whilst there is no measurable asymmetry in the results from rotating the model through  $90^\circ$  of roll, there are small but significant differences between the results at positive and negative values of incidence: the differences also vary apparently randomly with Mach number\*. This suggests that the differences are due to non-uniform flow in the wind tunnel rather than to any asymmetry in the geometry of the model. Comparisons with a few measurements obtained with the model stationary, whilst taking schlieren photographs, would suggest, however, that they may be due in part to the effect of taking readings with  $\theta$  slowly varying. Since this

---

\* The differences were particularly marked during the tests at  $M = 1.2$  and varying Reynolds number (results not presented here), where a considerable and progressive zero shift in  $C_m$  was observed with increasing Reynolds number.



asymmetry does not significantly affect the accuracy of the derived values of centre of pressure, and since any correction to the basic data would at best be doubtful, the results are presented as measured.

The pitching moment coefficients for configuration 02 are presented in Figs.11-13. The addition of the external fittings results in a reduction in the values of  $C_m$  at all test conditions, the reduction being a maximum with the pipes nearest to the horizontal plane, i.e.  $\phi \approx -5^\circ$ , and a minimum with the pipes near the vertical plane.

The variations with  $\theta$  and  $\phi$  of the centre of pressure  $-C_m/C_Z$ , equal to the distance in maximum body diameters of the centre of pressure ahead of the moment reference point of Fig.2a, are presented in Fig.14. The fittings result in a small increase in the rate of the rearward movement of the centre of pressure with increasing  $|\theta|$  and a general rearward displacement of the centre of pressure. The nett effect of the external fittings on the longitudinal characteristics of the launcher is a general small increase in stability which is a maximum with the pipes near the horizontal plane and a minimum with the pipes near the vertical plane.

The rolling moment and lateral forces measured on the axisymmetric configuration 01 do not vary measurably with  $\theta$  at any test condition, but they do exhibit small zero errors which vary with  $\phi$ , but which are all well within the estimated accuracy of the data (see section 3.5).

The rolling moments and lateral forces produced by the addition of the external fittings are small and not significantly different at the three Mach numbers investigated. The rolling moment and lateral force coefficients,  $C_\ell$ ,  $C_Y$  and  $C_n$ , measured on configuration 02 at  $M = 1.5$ , as typical of the Mach numbers tested, are presented in Figs.15-17. It is seen that the curves do not in general pass through the origin but that the values at  $\theta = 0^\circ$  are generally within the estimated accuracy of the data. The differences between the measured values of  $C_\ell$  at positive and negative values of incidence are also thought to be due to experimental errors and are also within the estimated accuracy of the results.

At small values of  $\theta$  the addition of the external fittings produces no measurable rolling moments (Fig.15) whilst at the higher values of  $\theta$  considered the launcher is stable in roll with the pipes near the horizontal plane ( $\phi \approx -10^\circ$ ).

Varying the Reynolds number from  $0.98 \times 10^6$  to  $1.64 \times 10^6$  at  $M = 1.2$  has no measurable effect on the forces on the model other than to give a (probably spurious) zero shift on  $C_m$  as discussed earlier in this section. It is estimated, however, that the fittings were always largely within the boundary layer on the model and it is possible that at the much higher Reynolds numbers of flight (typically  $20 \times 10^6$  - see Fig.4) the appreciably thinner boundary layers will lead to some increase in the effects of the fittings.

The base pressure was not measurably affected by changes in roll angle for either configuration, but the addition of the external fittings did significantly decrease its absolute value. The variation of base pressure with incidence is presented in Fig.18: the highest value of base pressure is obtained close to zero incidence.

All the measured forces on the launcher due to the addition of the external fittings are consistent with the pipes on the windward side developing more lift than the pipes on the leeward side, and with the centre of pressure of this additional lift acting behind the moment reference point (as we might expect from the geometry of the launcher).

## 5 CONCLUSIONS

The variations of normal force and pitching moment with angle of incidence, measured on the axisymmetric configuration 01, are smooth but non-linear over the range of conditions considered and the configuration is longitudinally stable.

The addition of the external fittings has a small but significant effect on the measured forces, which is due mainly to the external pipes. The effect of the external fairings is comparatively small.

The external fittings increase the normal force, the slope of the normal force curve and the longitudinal stability of the model at all test conditions. The effects are a maximum with the pipes in approximately the horizontal plane ( $\phi = -5^\circ$  to  $-10^\circ$ ), where the model is also stable in roll, and a minimum with the pipes in approximately the vertical plane. The additional forces are consistent with the pipes on the windward side developing more lift than the pipes on the leeward side of the model and with the centre of pressure of this additional lift acting behind the moment reference point. No measurable differences were observed between the results at positive and negative values of incidence for either configuration.

The value of the base pressure was significantly decreased, at all values of incidence investigated, by the addition of external fittings. The base pressure was not measurably affected by changes in roll angle for either configuration.

SYMBOLS

$C_\ell$	rolling moment coefficient = $\ell/qSd$
$C_m$	pitching moment coefficient = $m/qSd$
$C_n$	yawing moment coefficient = $n/qSd$
$C_{pb}$	base pressure coefficient = (base pressure - free-stream static pressure)/q
$C_Y$	side force coefficient = $Y/qS$
$-C_Z$	normal force coefficient = $-Z/qS$
$d$	maximum body diameter
$\ell$	rolling moment = moment about OX, positive starboard side down (Fig.3)
$m$	pitching moment = moment about OY, positive nose up (Fig.3)
$M$	free-stream Mach number
$M_N$	nominal Mach number = Mach number setting of the walls of the wind tunnel
$n$	yawing moment = moment about OZ, positive nose to starboard (Fig.3)
OX, OY, OZ	right-handed cartesian axes with the origin 0 at the moment reference point, OX along the model axis and OZ in the plane containing the model axis and the wind vector (i.e. axes move with the model in pitch but not in roll). Directions etc. as given in Fig.3
$q$	kinetic pressure of the free stream
$R_d$	Reynolds number based on free-stream conditions and the maximum body diameter, $d$
$S$	reference area = $\pi d^2/4$
$X_{cp}$	distance of the centre of pressure forward of the moment reference point = $d \times C_m/C_Z$
$Y$	side force = force on model in direction OY (Fig.3)
$-Z$	normal force = force on model in direction -OZ (Fig.3)
$\theta$	angle between the model axis and the wind vector
$\Delta\theta$	a correction to $\theta$
$\phi$	angle between the model roll datum and OY (see Figs.2 and 3)

REFERENCES

<u>No.</u>	<u>Author</u>	<u>Title</u>
1	Staff of Space Department	A small satellite launcher based on Black Knight technology. Unpublished MOD(PE) material
2	Staff of Space Department	The Black Arrow satellite launching vehicle. RAE Technical Report 69068 (ARC 31547) (1969)
3	J. B. Scott	The Black Arrow launching vehicle - an assessment of the performance of advanced versions. RAE Technical Report 65072 (ARC 26986) (1965)
4	E. R. Van Driest C. B. Blumer	Effect of roughness on transition in supersonic flow. AGARD Report 255 (1960)



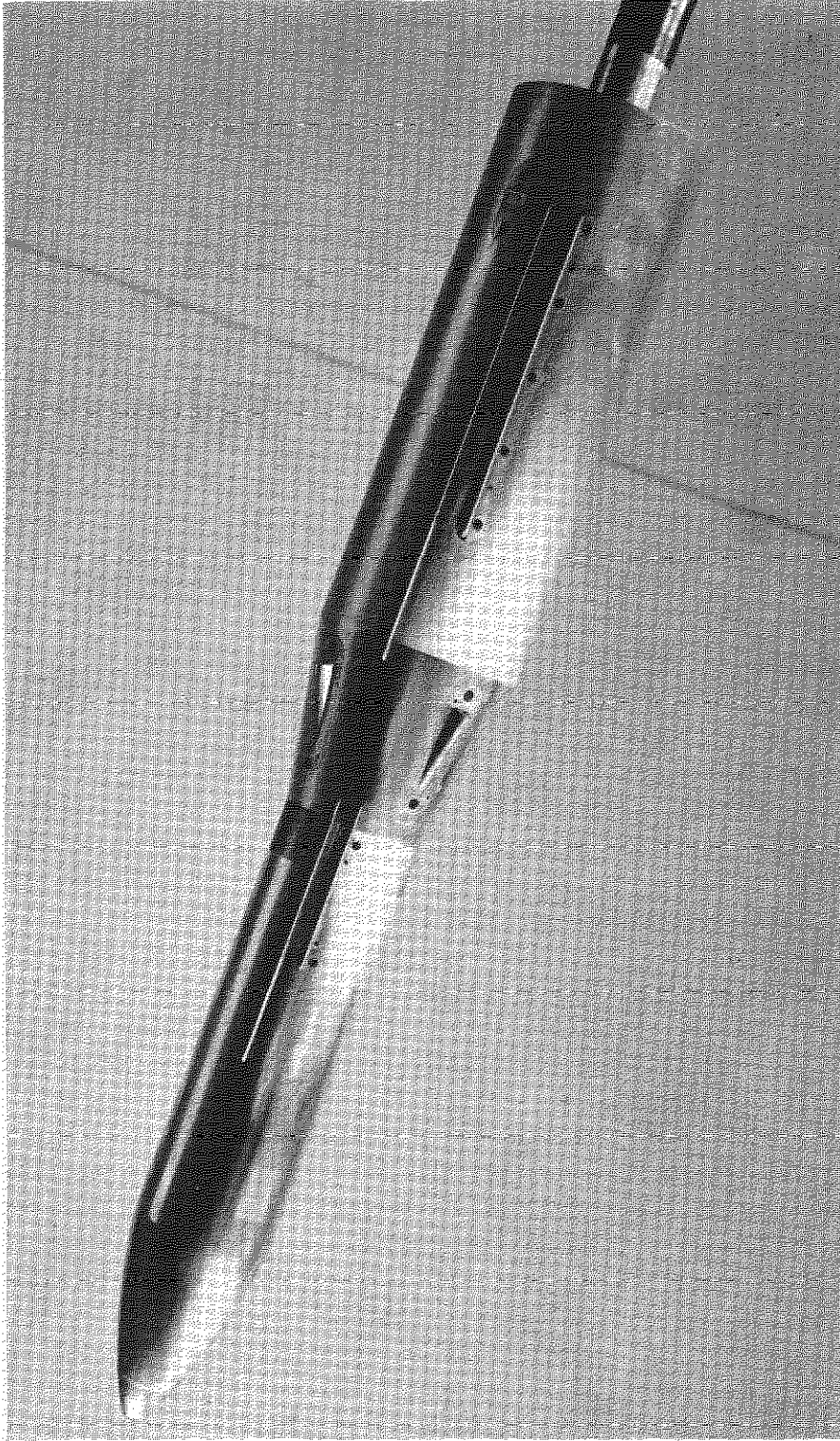
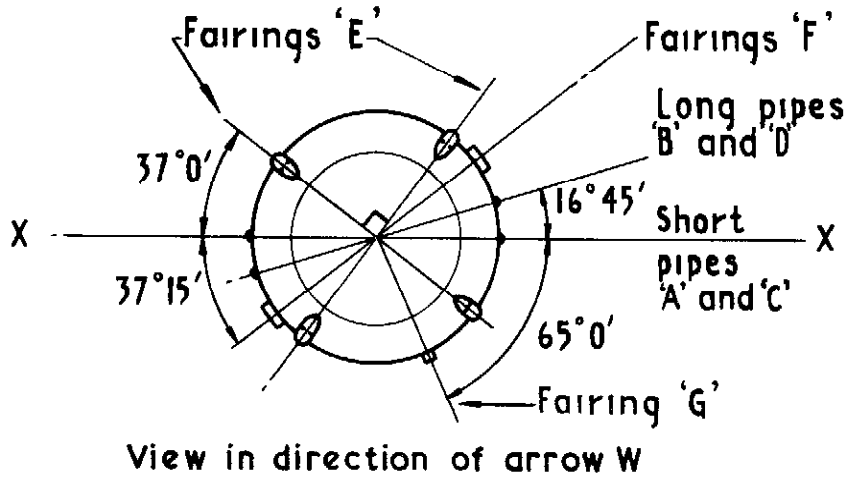
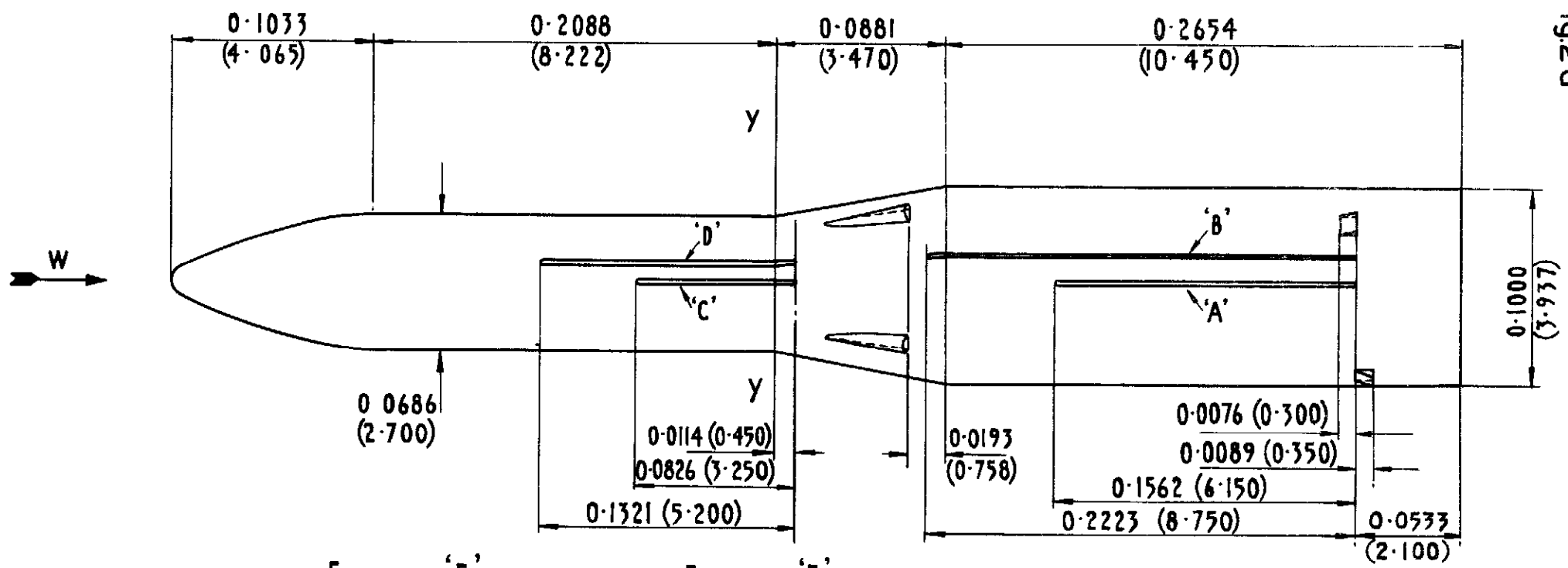


**Fig.1 The model mounted in the wind tunnel (configuration 02)**

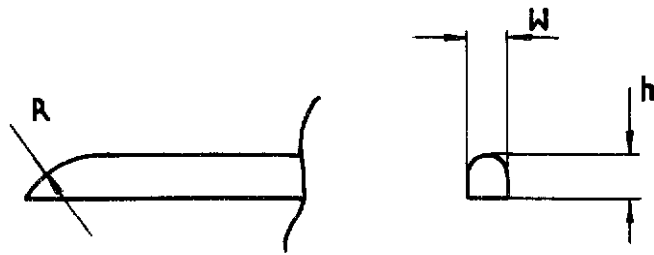


Note  
 (1) X-X zero roll datum  
 (2) Moment reference point at intersection of Y-Y with axis of model

Scale -  $\frac{1}{3}$  model scale  
 dimensions in m (in)

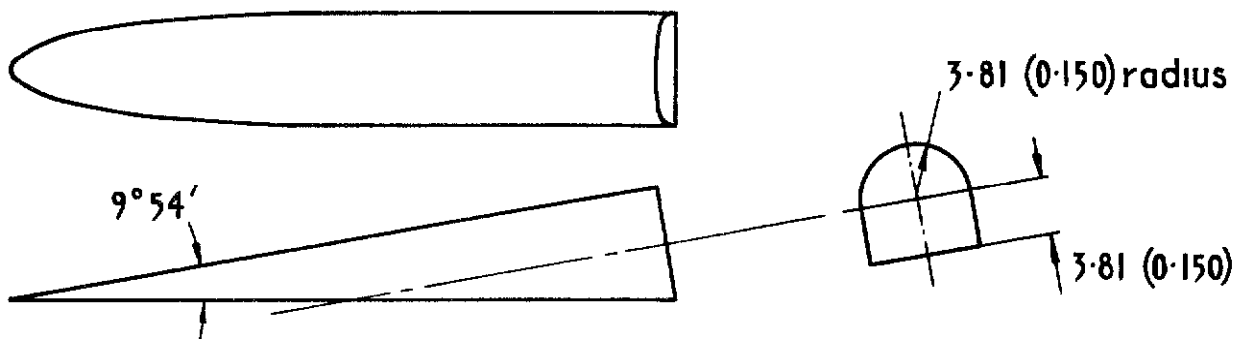
Fig2a General arrangement of the model





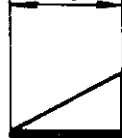
Pipe	h	W	R	Length
A	350 (0.1379)	3.16 (0.1246)	7.94 (0.3125)	156.2 (6.150)
B	2.82 (0.1110)	2.54 (0.0999)	6.35 (0.250)	222.3 (8.750)
C	2.22 (0.0875)	1.90 (0.0749)	6.35 (0.250)	82.6 (3.250)
D	2.82 (0.1110)	2.54 (0.0999)	6.35 (0.250)	132.1 (5.200)

i Pipes /conduits (2 off each)

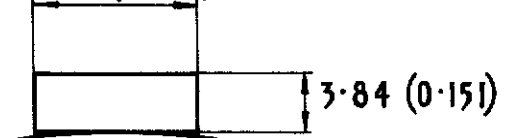


ii Fairings 'E' on flare (4 off)

7.62 (0.300)

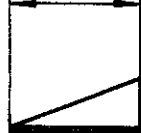


10.82 (0.426)



iii Fairings 'F' on rear-body (2 off)

8.89 (0.350)



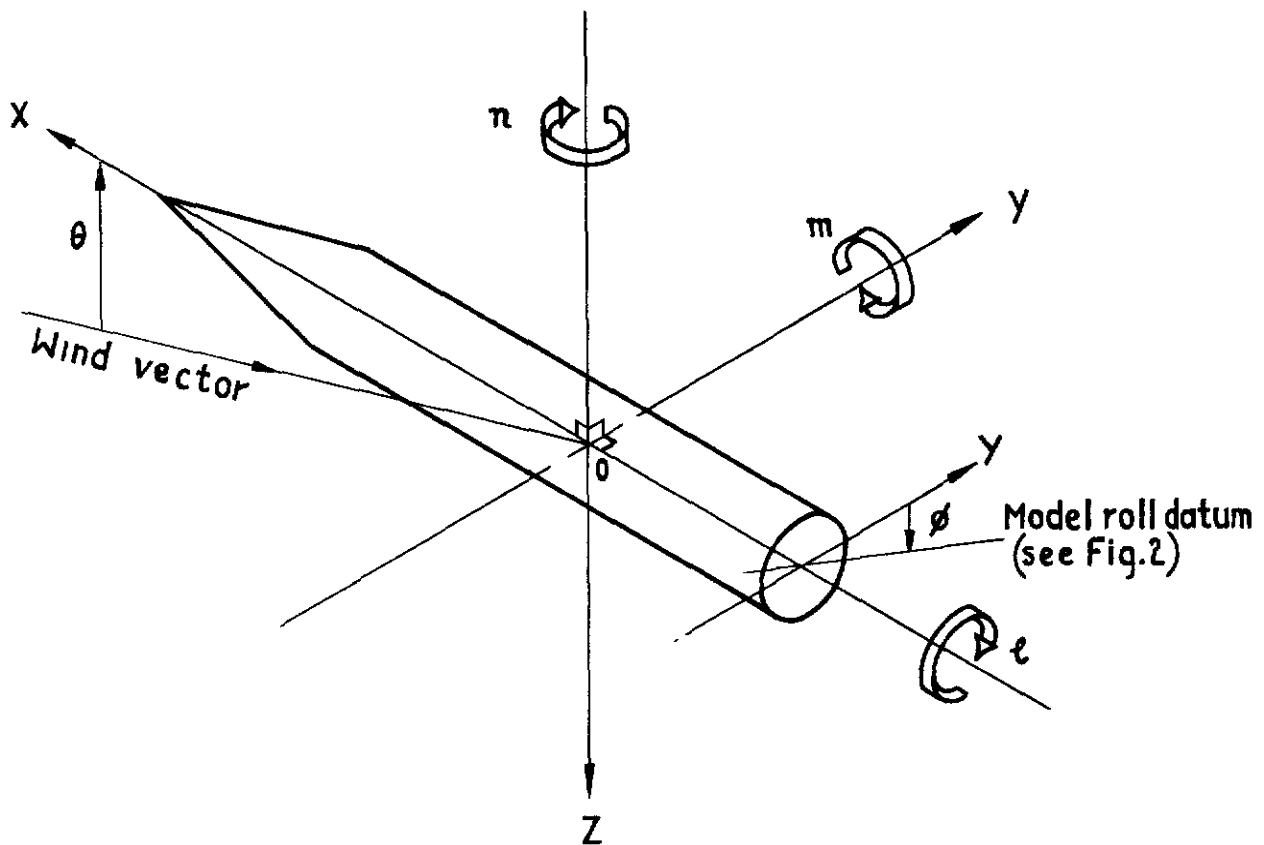
5.08 (0.200)



iv Fairing 'G' on rear-body (1 off)

Scale approx twice model size  
 Dimensions in mm (inch)  
 For letters A to G see Fig.2a

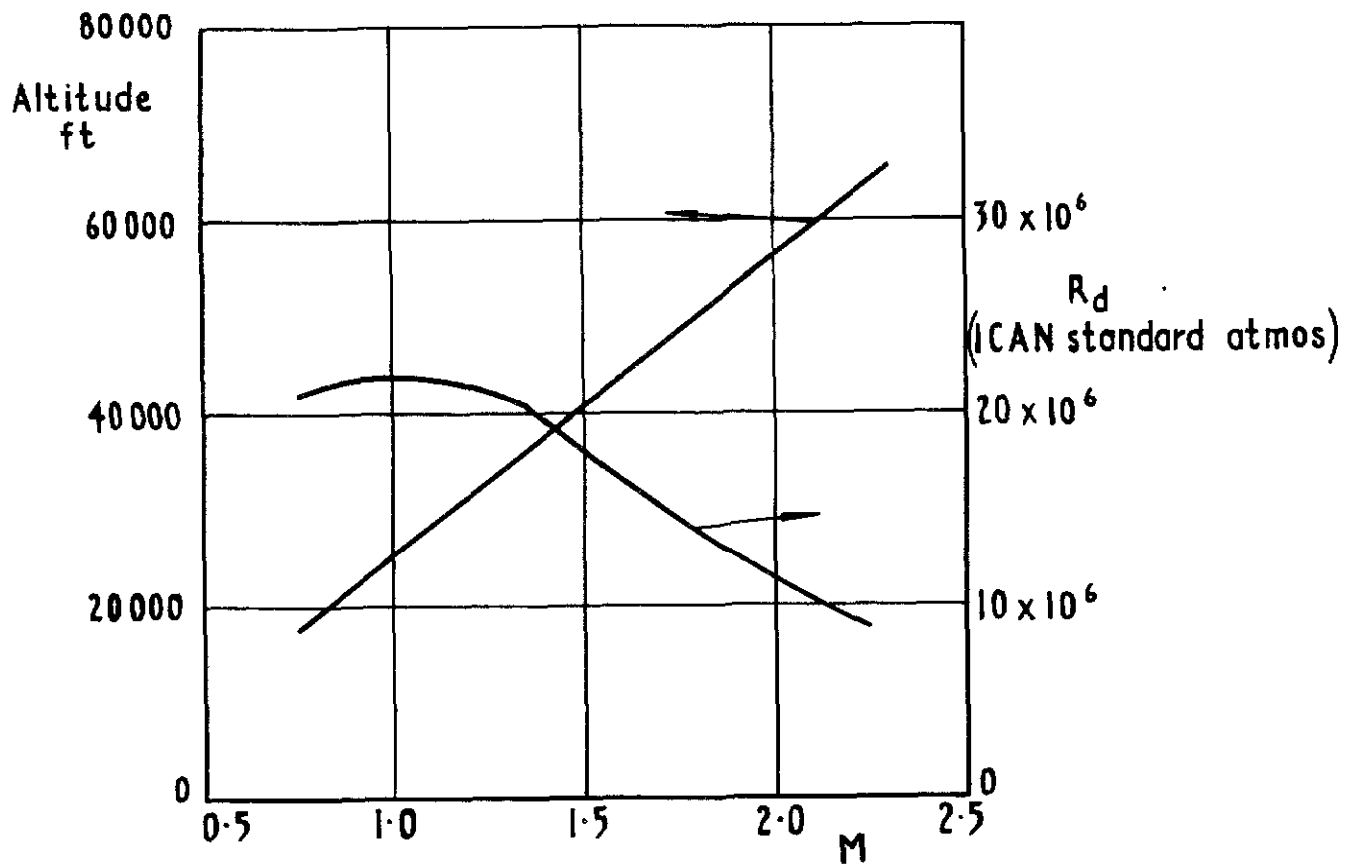
Fig.2b Details of external fittings



$Ox, Oy, Oz$ —Right handed cartesian axes with origin  $O$  at moment reference point (figure 2)  
 The axes move with the model in pitch,  $\theta$ , but not in roll,  $\phi$   
 Forces and moments acting on model are positive in directions shown

Fig.3 Resolved body axes

TR 72061



Model test conditions:  $R_d = 1.31 \times 10^6$

Fig.4 Design flight path

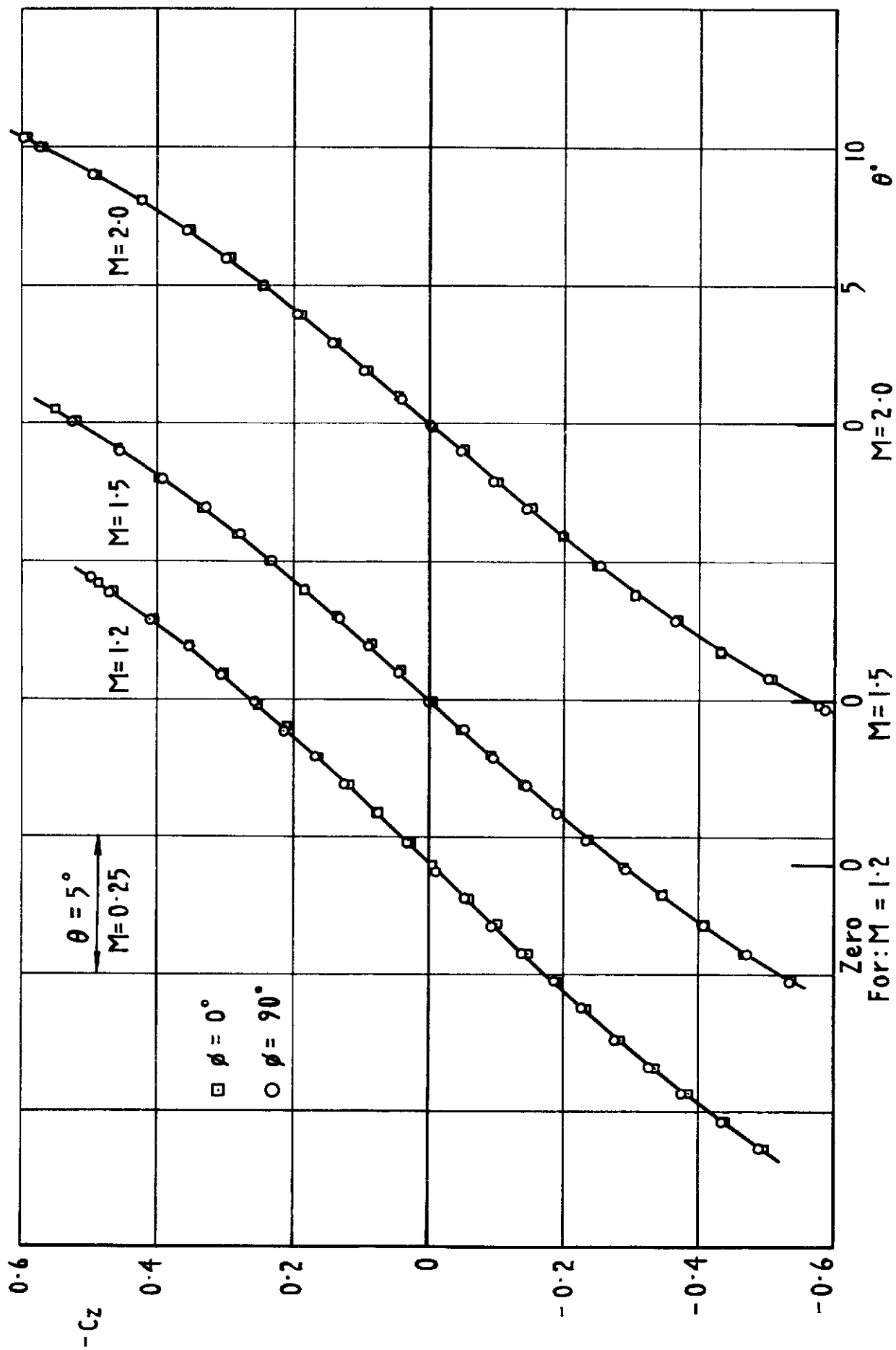


Fig.5 Variation of normal force with incidence and roll  
 Config OI  $R_d = 1.31 \times 10^6$

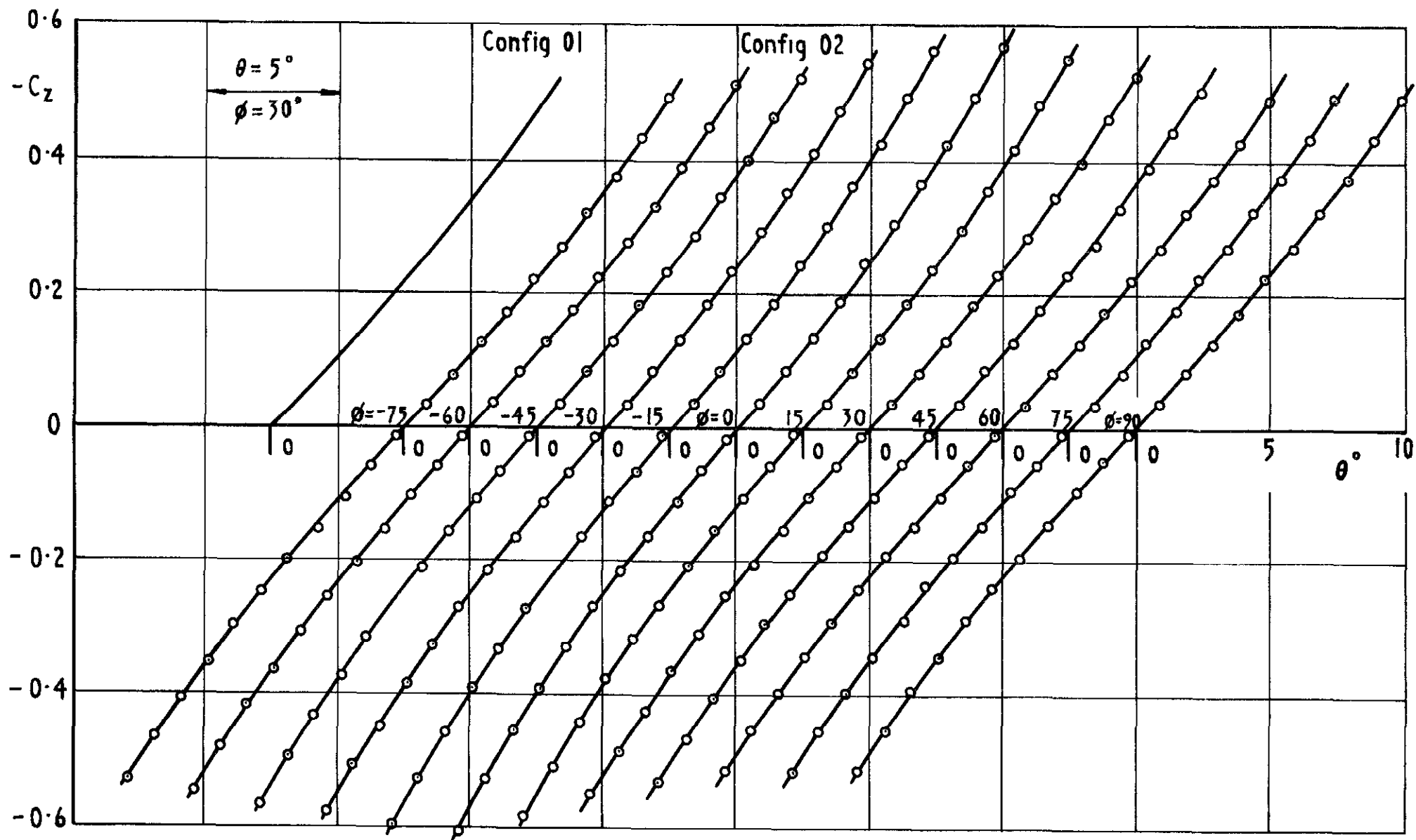


Fig.6 Variation of normal force with incidence and roll  
 $M=1.2 \quad R_d = 1.31 \times 10^6$

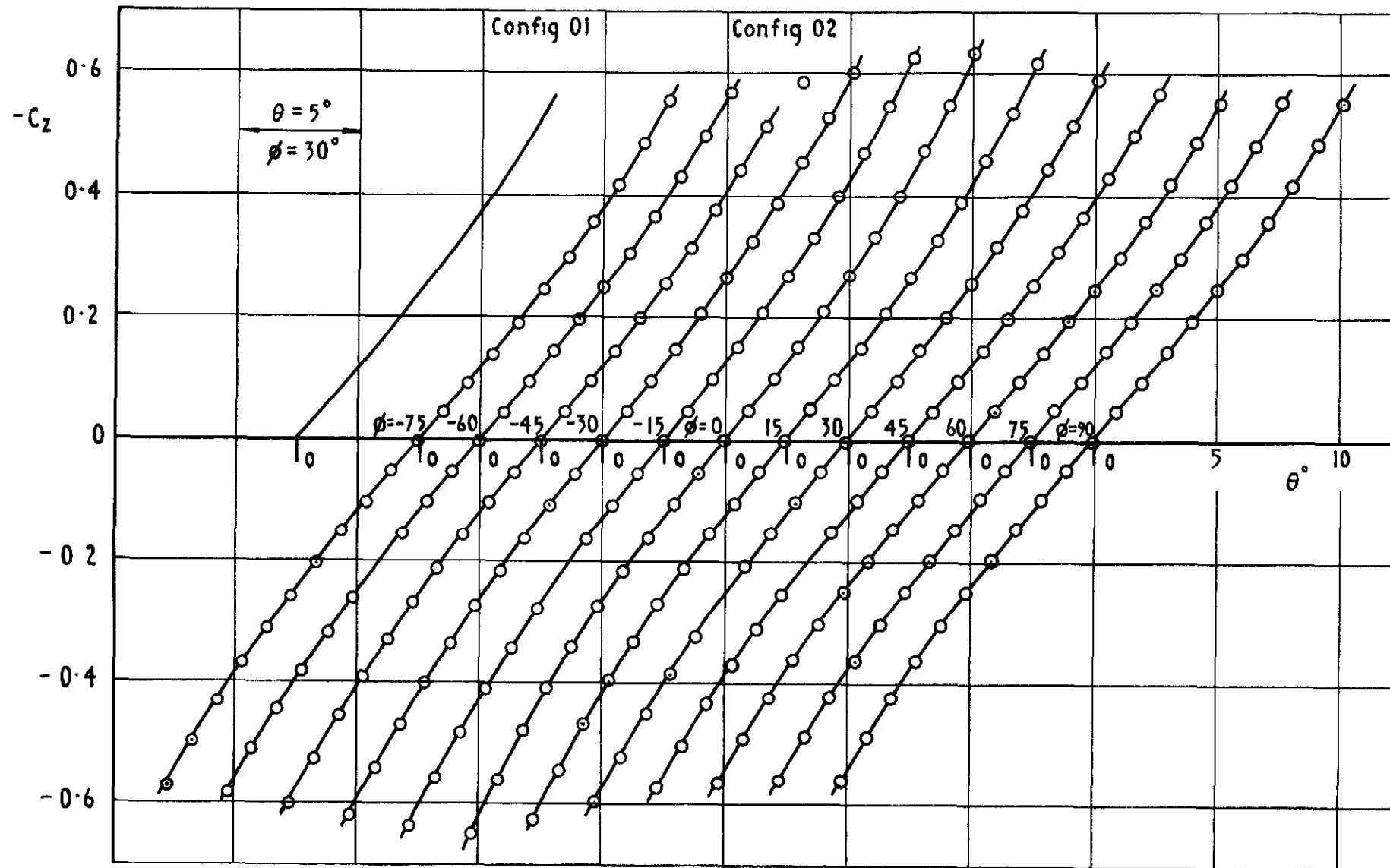


Fig.7 Variation of normal force with incidence and roll  
 $M=1.5 \quad R_d = 1.31 \times 10^6$

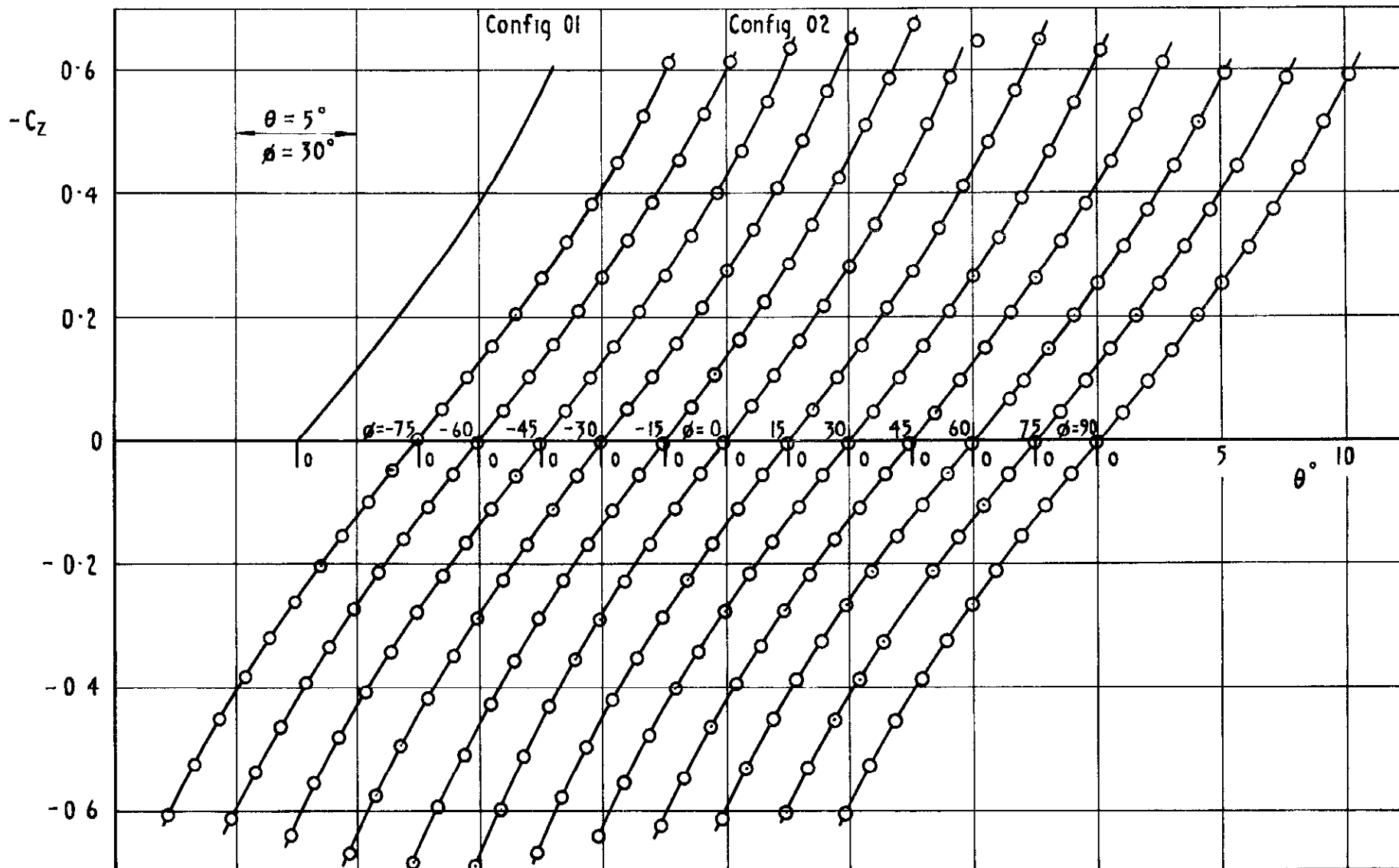


Fig.8 Variation of normal force with incidence and roll

$$M = 2.0 \quad R_D = 1.31 \times 10^6$$

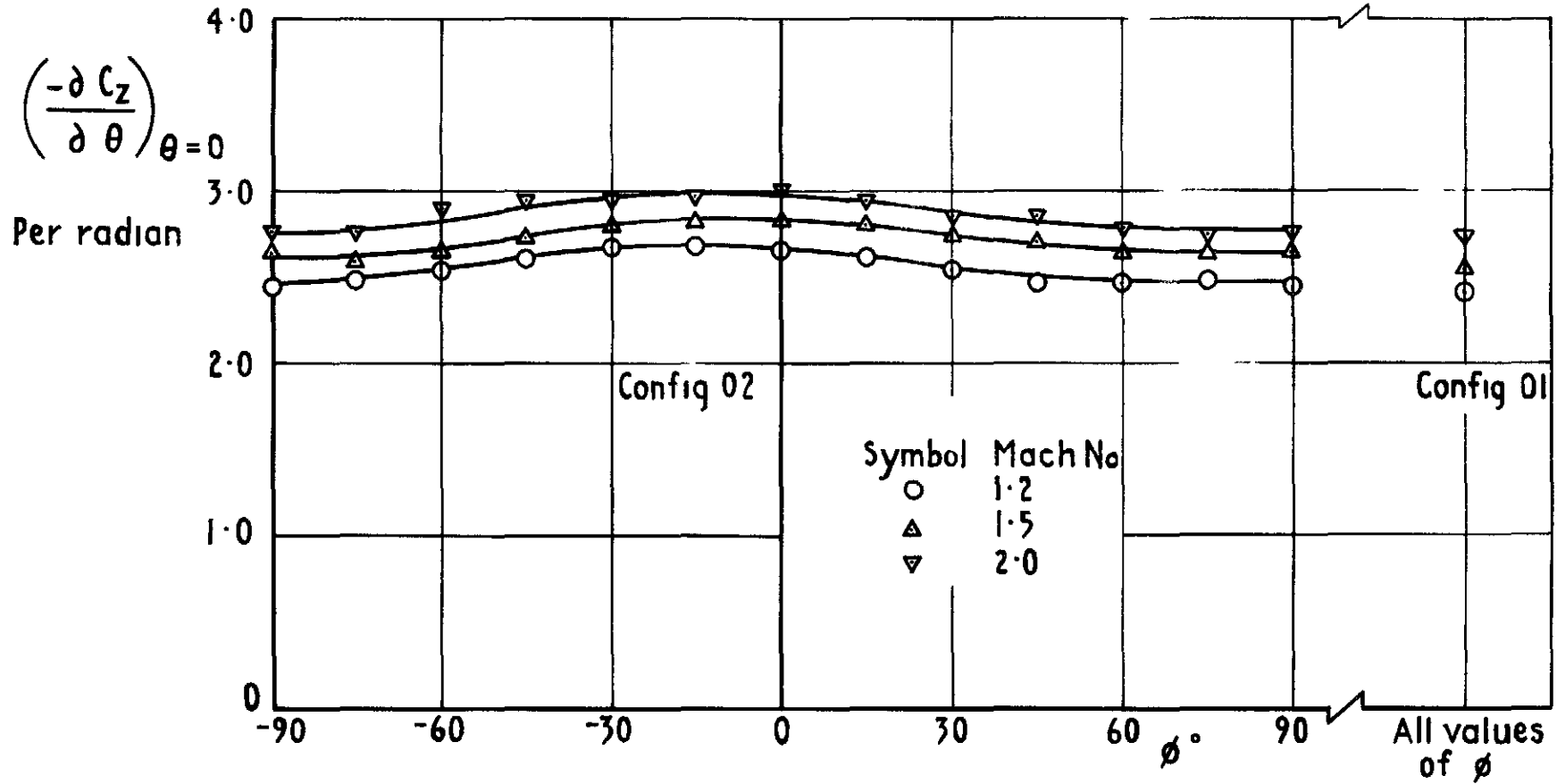


Fig.9 Slope of normal force curve at zero normal force  $R_d = 1.31 \times 10^6$



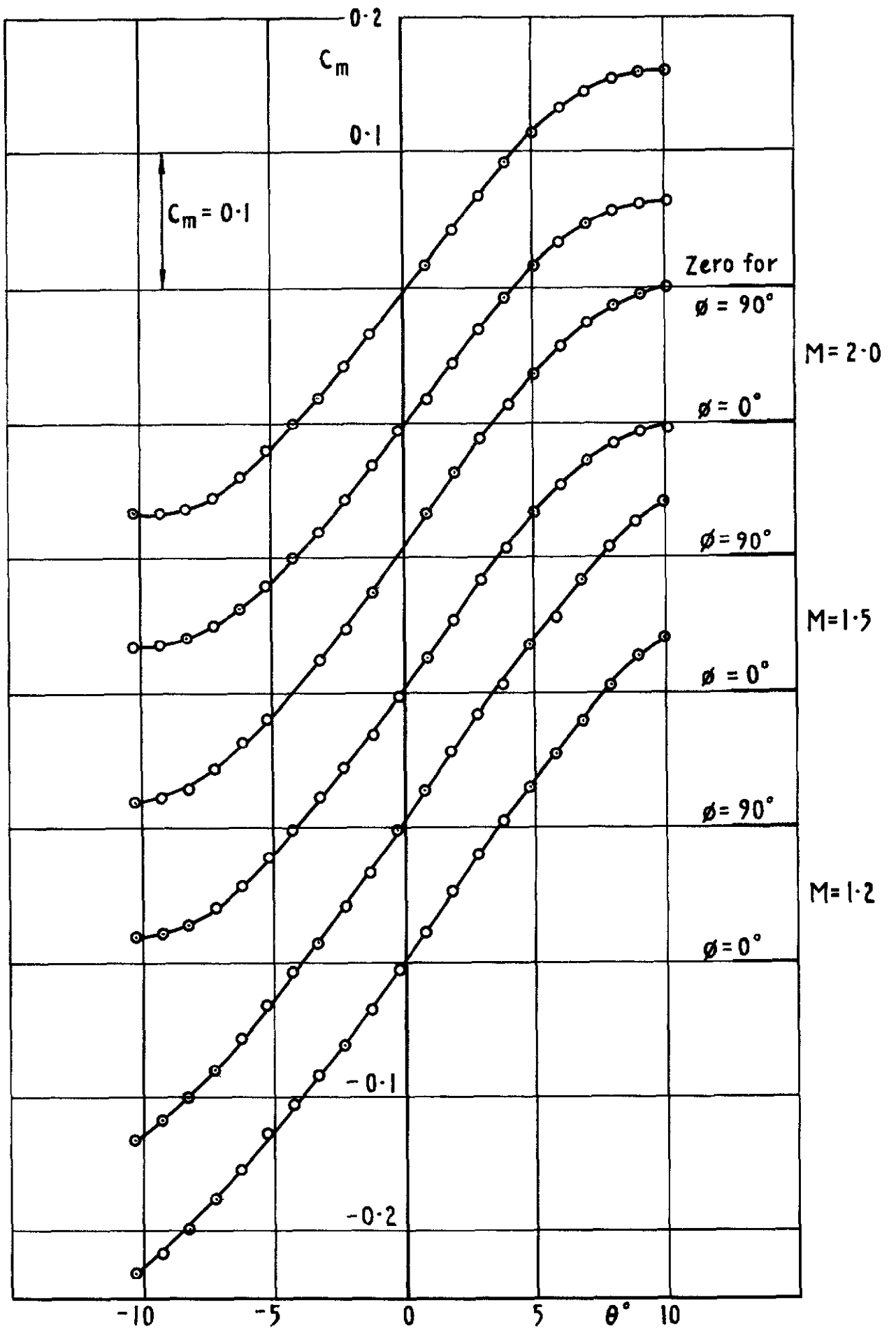


Fig 10 Variation of pitching moment with incidence and roll  
 Config OI  $R_D = 1.31 \times 10^6$

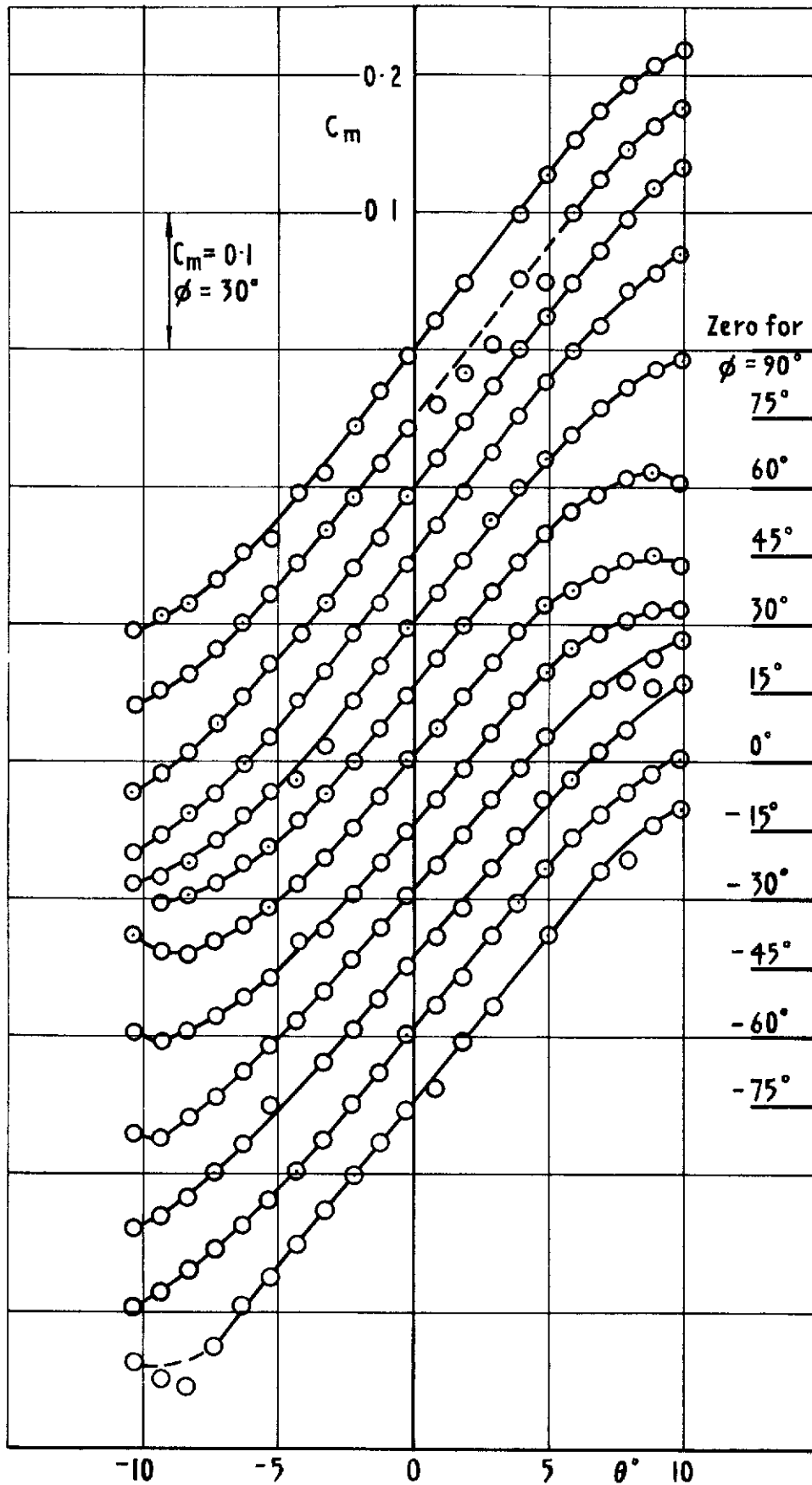


Fig. 11 Variation of pitching moment with incidence and roll  
 Config O2  $M = 1.2$   $R_d = 1.31 \times 10^6$

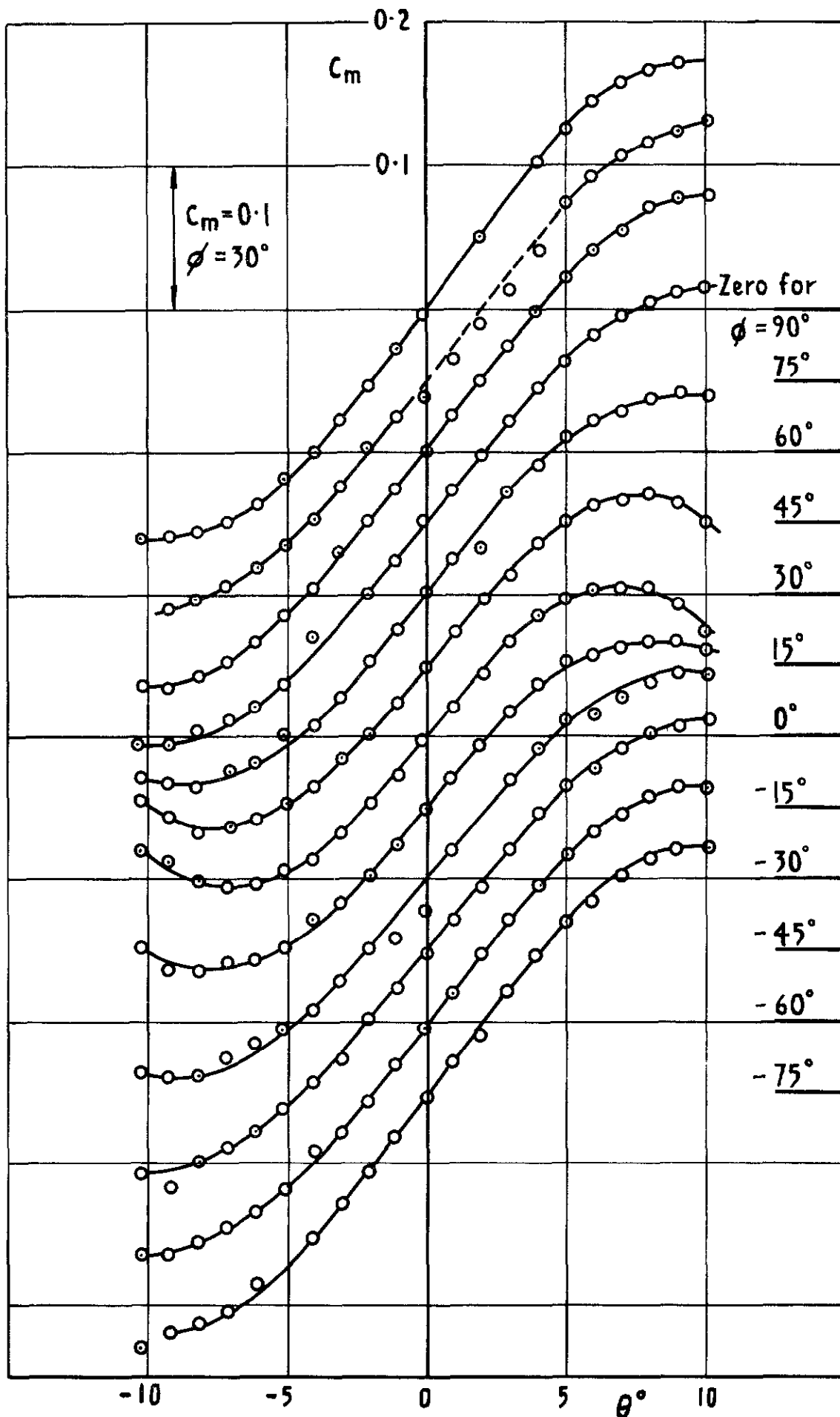


Fig.12 Variation of pitching moment with incidence and roll  
 Config O2  $M = 1.50$   $R_d = 1.31 \times 10^6$

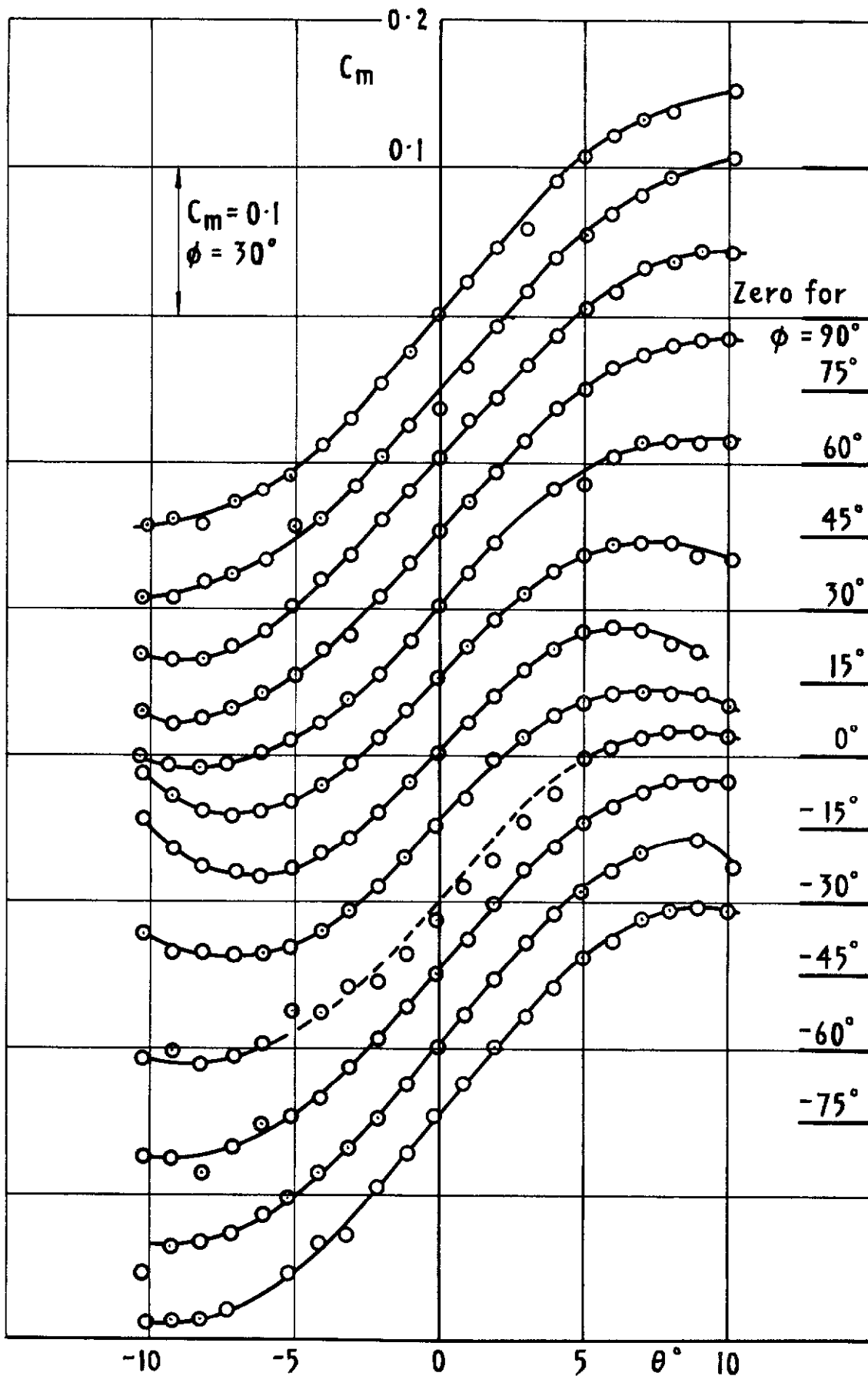
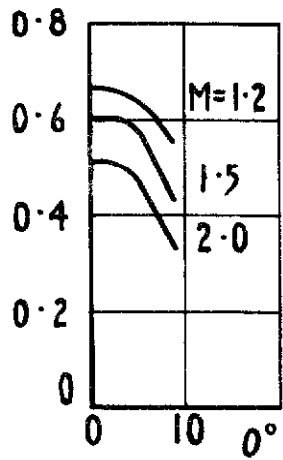


Fig.13 Variation of pitching moment with incidence and roll  
 Config O2  $M = 2.0$   $R_d = 1.31 \times 10^6$

Configuration 01

Centre of pressure  
 $\frac{X_{cp}}{d}$



Configuration 02

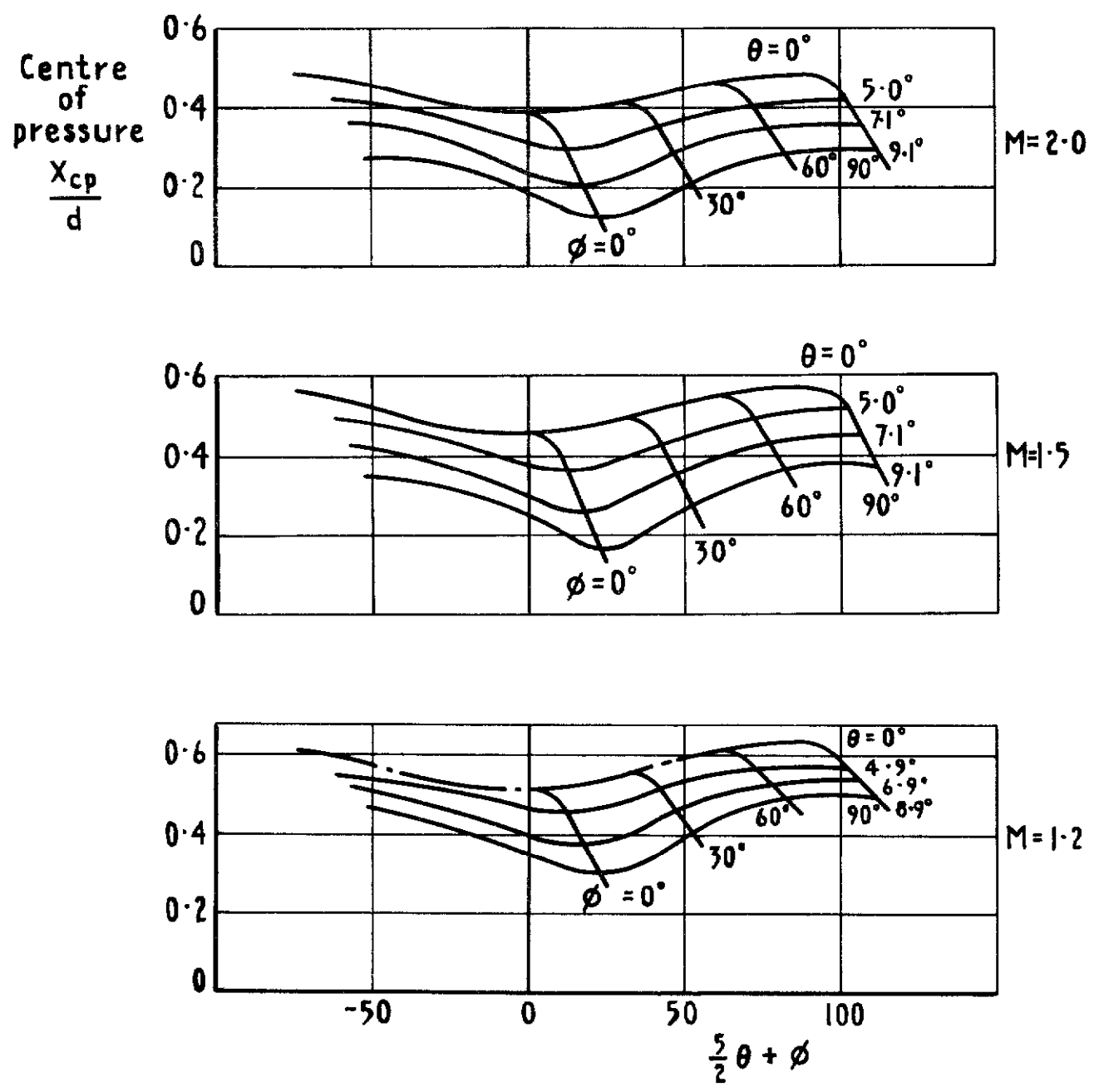


Fig.14 Position of the centre of pressure forward of the moment reference point (see Fig. 2a)  $R_d = 1.31 \times 10^6$

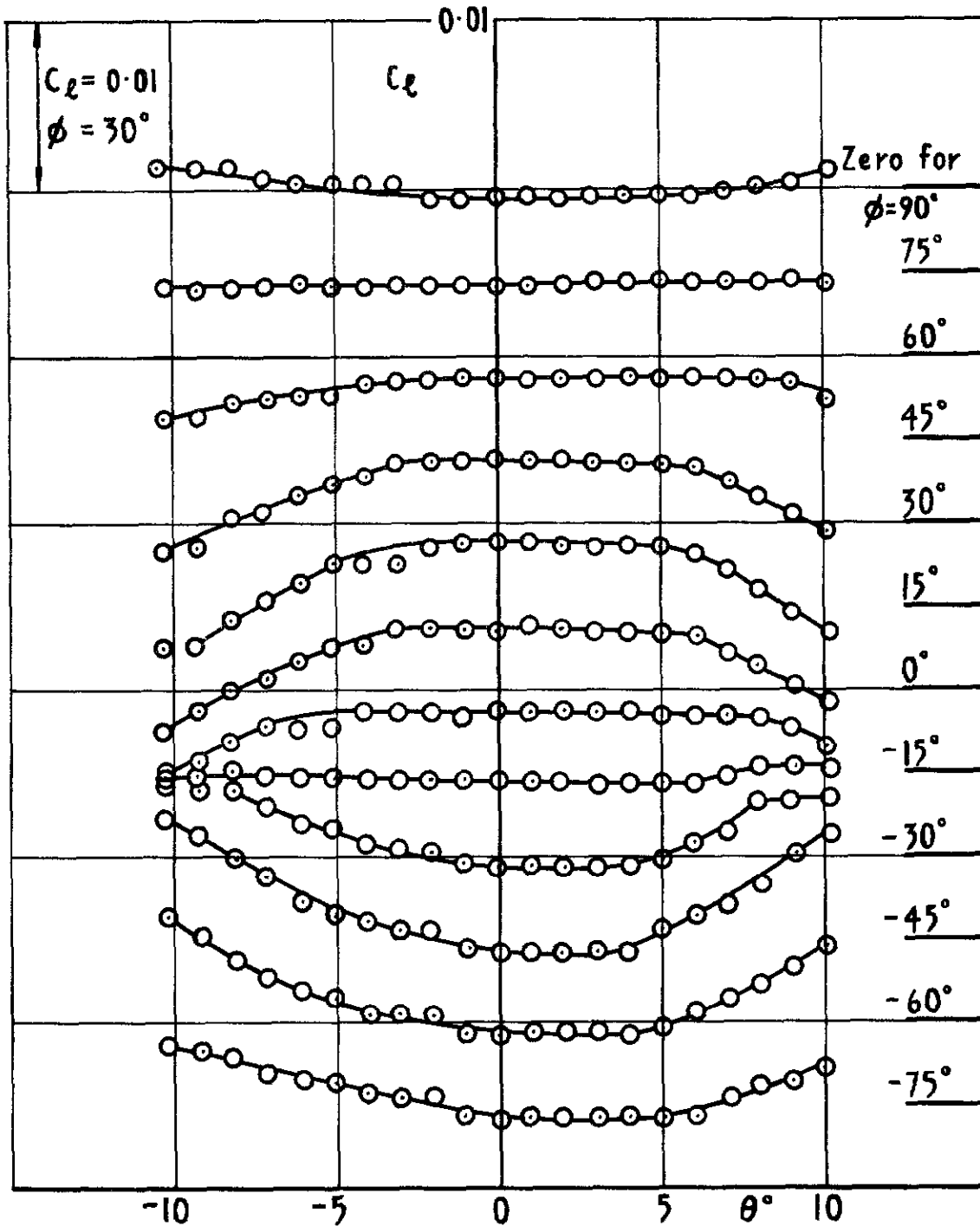


Fig.15 Variation of rolling moment with incidence and roll  
 Config O2  $M = 1.5$   $R_d = 1.31 \times 10^6$

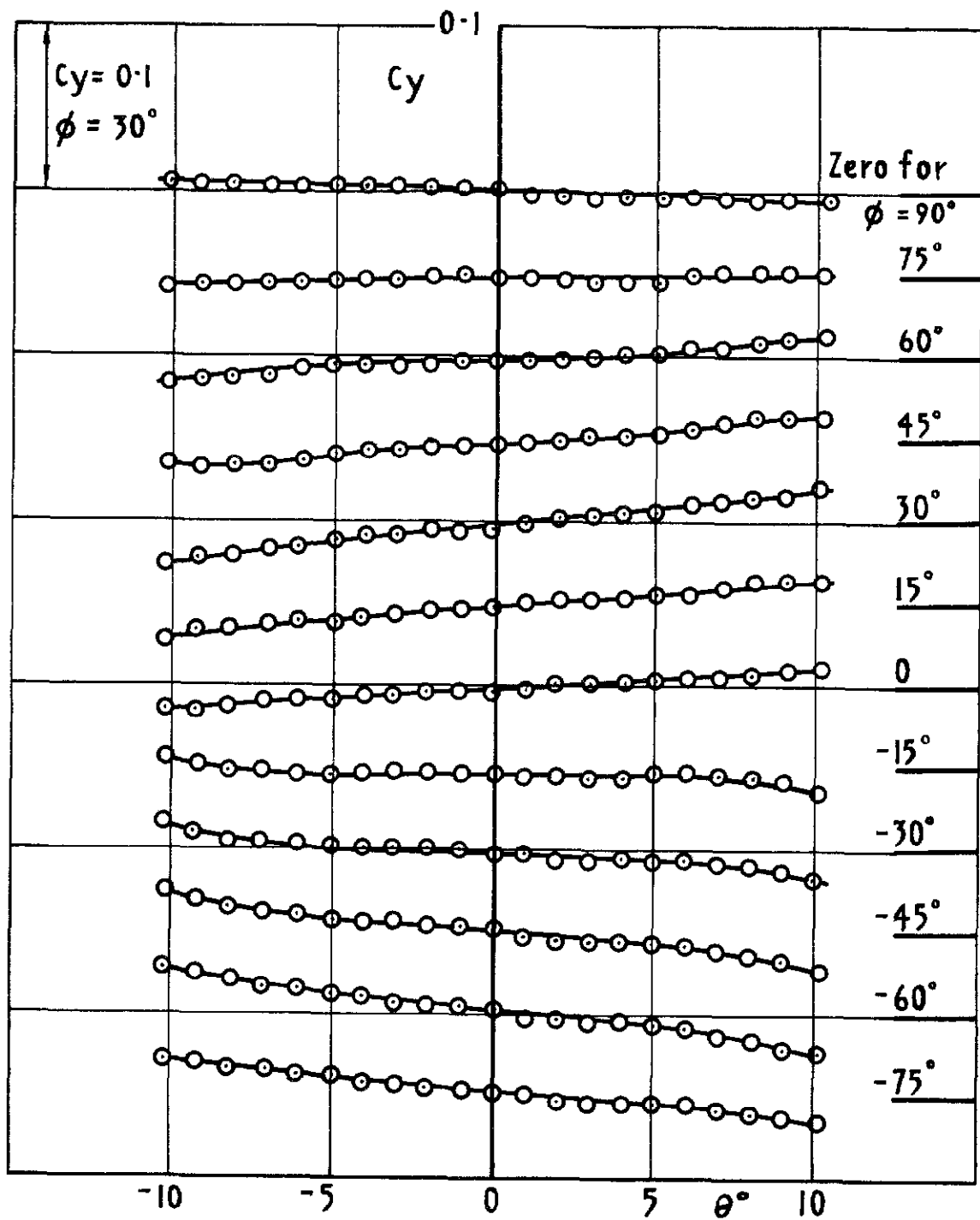


Fig.16 Variation of side force with incidence and roll  
 Config O2  $M=1.5$   $R_d=1.31 \times 10^6$

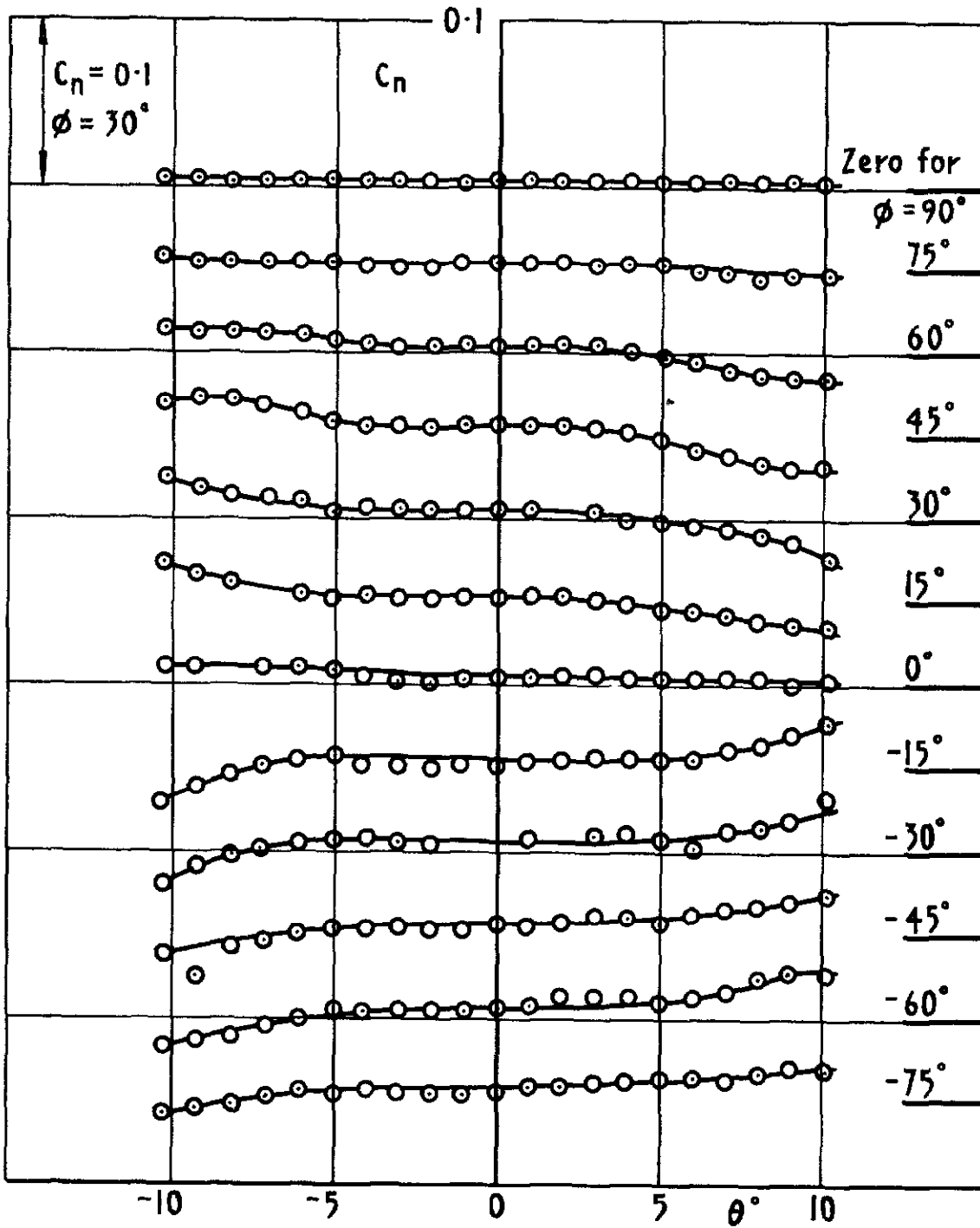


Fig.17 Variation of yawing moment with incidence and roll  
 Config O2  $M=1.5$   $R_d = 1.31 \times 10^6$



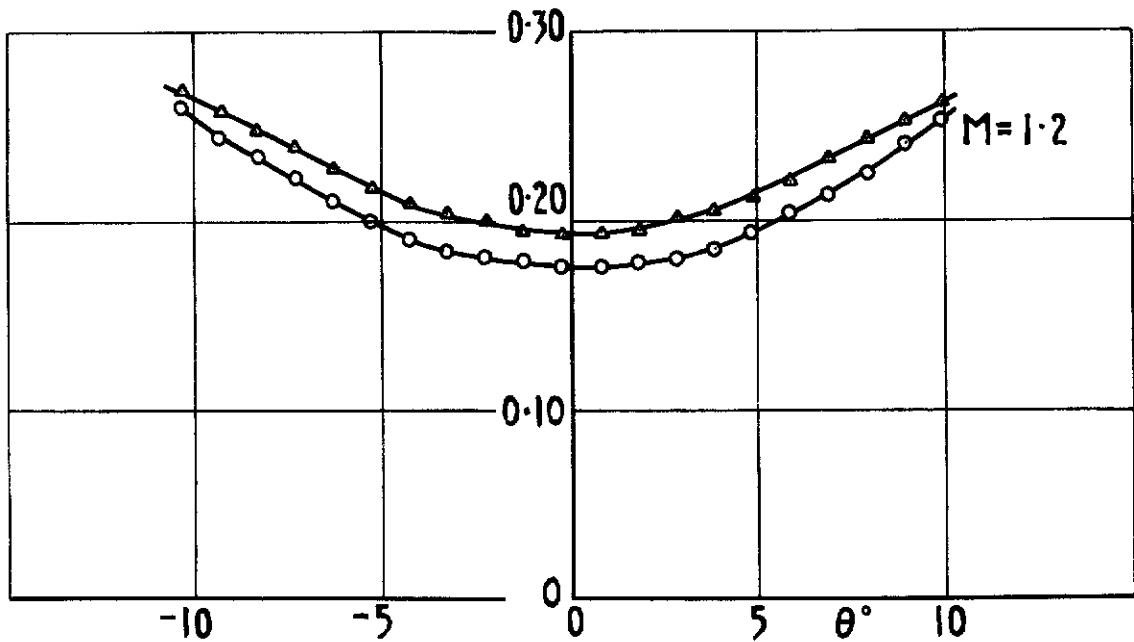
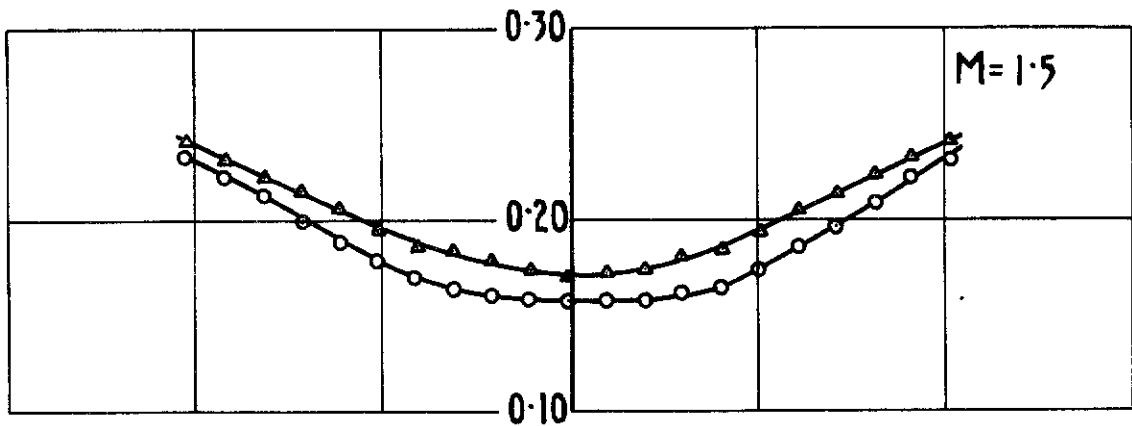
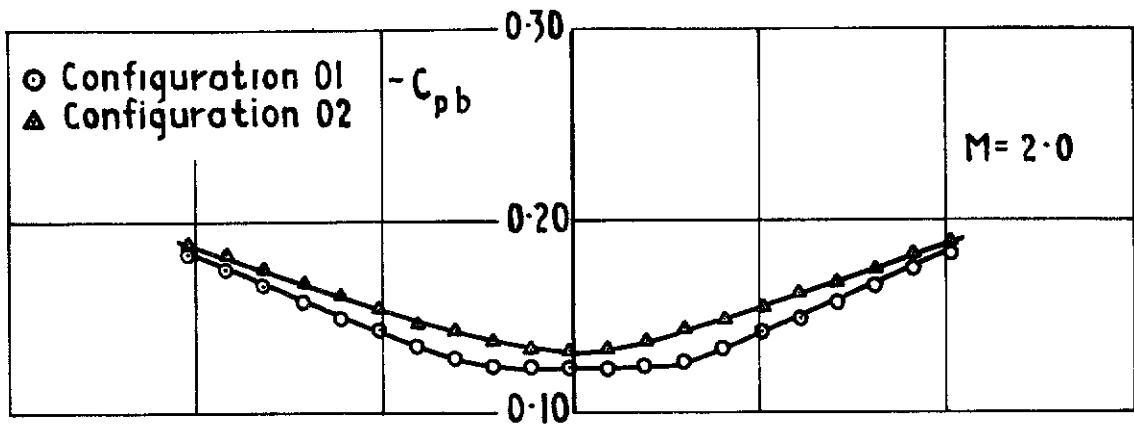


Fig.18 Variation of base pressure at zero roll with incidence  $R_d = 1.31 \times 10^6$



ARC CP No 1249  
March 1972

629.192 21  
533 6 013 11  
533.6 071  
533 6 011 5

Hall, J R.

WIND TUNNEL FORCE MEASUREMENTS ON A  
1/20 SCALE MODEL OF BLACK ARROW AT  
MACH NUMBERS OF 1.2, 1.5 AND 2.0

The forces measured on a 1/20 scale model of Black Arrow at Mach numbers of 1.2, 1.5 and 2.0 and at a Reynolds number, based on the maximum body diameter, of  $1.31 \times 10^6$  are presented. The effects of the external fittings are deduced and the results are discussed.

These abstract cards are inserted in Technical Reports for the convenience of Librarians and others who need to maintain an Information Index

----- Cut here -----

ARC CP No.1249  
March 1972

629.192.21  
533 6 013 11  
533.6 071  
533 6 011 5

Hall, J R

WIND TUNNEL FORCE MEASUREMENTS ON A  
1/20 SCALE MODEL OF BLACK ARROW AT  
MACH NUMBERS OF 1.2, 1.5 AND 2.0

The forces measured on a 1/20 scale model of Black Arrow at Mach numbers of 1.2, 1.5 and 2.0 and at a Reynolds number, based on the maximum body diameter, of  $1.31 \times 10^6$  are presented. The effects of the external fittings are deduced and the results are discussed.

ARC CP No 1249  
March 1972

629 192 21  
533 6 013 11  
533.6.071  
533 6 011 5

Hall, J R

WIND TUNNEL FORCE MEASUREMENTS ON A  
1/20 SCALE MODEL OF BLACK ARROW AT  
MACH NUMBERS OF 1.2, 1.5 AND 2.0

The forces measured on a 1/20 scale model of Black Arrow at Mach numbers of 1.2, 1.5 and 2.0 and at a Reynolds number, based on the maximum body diameter, of  $1.31 \times 10^6$  are presented. The effects of the external fittings are deduced and the results are discussed.

----- Cut here -----

DETACHABLE ABSTRACT CARDS

DETACHABLE ABSTRACT CARDS





© *Crown copyright*  
**1973**

Published by  
HER MAJESTY'S STATIONERY OFFICE

To be purchased from  
49 High Holborn, London WC1 V 6HB  
13a Castle Street, Edinburgh EH2 3AR  
109 St Mary Street, Cardiff CF1 1JW  
Brazenose Street, Manchester M60 8AS  
50 Fairfax Street, Bristol BS1 3DE  
258 Broad Street, Birmingham B1 2HE  
80 Chichester Street, Belfast BT1 4JY  
or through booksellers